ROYAL SOCIETY
OF CHEMISTRY

PAPER

Synthesis of wafer-scale uniform molybdenum disulfide films with control over the layer number using a gas phase sulfur precursor†

Youngbin Lee,‡[a] Jinhwan Lee,‡[b] Hunyoung Bark,[a] Il-Kwon Oh,[c] Gyeong Hee Ryu,[d]
Zonghoon Lee,[d] Hyungjun Kim,[c] Jeong Ho Cho,[a] Jong-Hyun Ahn*[c]
and Changgu Lee*[abe]

We describe a method for synthesizing large-area and uniform molybdenum disulfide films, with control over the layer number, on insulating substrates using a gas phase sulfuric precursor (H_2S) and a molybdenum metal source. The metal layer thickness was varied to effectively control the number of layers (2 to 12) present in the synthesized film. The films were grown on wafer-scale Si/SiO_2 or quartz substrates and displayed excellent uniformity and a high crystallinity over the entire area. Thin film transistors were prepared using these materials, and the performances of the devices were tested. The devices displayed an on/off current ratio of 10^5, a mobility of 0.12 cm^2 V^{-1} s^{-1} (mean mobility value of 0.07 cm^2 V^{-1} s^{-1}), and reliable operation.

Atomically thin-layered materials have been extensively studied in an effort to harness their exotic physical properties that result from two-dimensional confinement.[1–3] These materials are suitable for practical electronic applications due to their planar geometry.[4] Graphene, in particular, has been examined for its electronic,[1,5–8] mechanical,[2] optical,[9–11] biological,[12] and chemical properties.[13] Although graphene shows promise for its utility in high-performance electronics owing to its high charge carrier mobility,[14] it is a zero-bandgap material and suffers from certain drawbacks that prevent its use in electronic devices. For example, it is difficult to use graphene to prepare digital integrated circuits because those devices require a bandgap exceeding 0.4 eV in order to achieve an acceptable performance for practical applications.[15] Some researchers have attempted to increase the bandgap in graphene, but the bandgap size is generally too small, and all efforts occur at the expense of its excellent properties.[16–19]

[a]*SKKU Advanced Institute of Nanotechnology (SAINT) and Center for Human Interface Nano Technology (HINT), Sungkyunkwan University, Suwon 440-746, Korea. E-mail: peterlee@skku.edu; Fax: +82-31-299-7930; Tel: +82-31-299-4844*

[b]*School of Mechanical Engineering, Sungkyunkwan University, Suwon 440-746, Korea*

[c]*School of Electrical and Electronic Engineering, Yonsei University, 50 Yonsei-Ro, Seodaemun-Gu, Seoul 120-749, Korea. E-mail: ahnj@yonsei.ac.kr; Fax: +82-2-313-2879; Tel: +82-2-2123-2776*

[d]*School of Mechanical and Advanced Materials Engineering, Ulsan National Institute of Science and Technology (UNIST), Ulsan 689-798, Korea*

[e]*Center for Integrated Nanostructure Physics (CINAP), Insistute for Basic Science (IBS), Sungkyunkwan University, Suwon 440-746, Korea*

† Electronic supplementary information (ESI) available: Schematic illustration of the CVD system and AFM and HRTEM measurements. See DOI: 10.1039/c3nr05993f

‡ Y. Lee and J. Lee contributed equally to this work.

Recent studies have explored the use of two-dimensional semiconducting materials, such as sulfides (MoS_2, WS_2, TiS_2, *etc.*) and selenides (GaSe, $NbSe_2$, In_2Se_3, *etc.*), for the preparation of thin film transistors (TFTs) and high-performance integrated circuits because these materials provide an intrinsic bandgap between 1 and 2 eV.[20] Molybdenum disulfide (MoS_2), in particular, has attracted attention due to its high mobility, which exceeds 200 cm^2 V^{-1} s^{-1}, and its on/off ratio of 10^8, which can meet the needs of many electronic applications.[21] In addition to having good electrical properties, atomically thin MoS_2 crystals exhibit excellent mechanical and optical properties that are useful for large-area applications, such as backplane TFTs for flexible and transparent displays. Utility in large-area synthesis techniques is essential for the application of MoS_2 materials in macroscopic electronic applications. Recently, several approaches based on chemical vapor deposition (CVD) have been reported. One of the most commonly used methods involves the reaction of the Mo metal with the sulfur precursor gas evaporated from a solid sulfur source.[22] Although this approach can facilitate the large-area synthesis of MoS_2 films over a length scale of a few inches, it can be difficult to control the number of layers and the uniformity of the layer distribution. Residual Mo atoms tend not to react and remain with the sulfur atoms. Another CVD method involved the use of MoO_3 in place of the Mo metal source. The resulting MoS_2 films exhibited relatively high crystallinity, a low concentration of residual MoO_3, and reasonable charge carrier mobility.[23–26] This method has several weaknesses: it is difficult to control the film thickness, and discontinuities are present between the crystals, producing a non-uniform charge carrier mobility.

Here, we present the development of a large-area synthesis method for preparing high-quality MoS_2 films using H_2S gas and a Mo metal source. This approach offers important advantages over other CVD methods, including (i) uniform layer thicknesses over a large substrate area, such as SiO_2 or quartz, up to the wafer scale and (ii) readily controllable film thickness by changing the thickness of the deposited metal source. We demonstrated the preparation of a large-area transferrable MoS_2 TFT array on a wafer. This technology offers important advantages over transparent semiconducting materials, such as oxide semiconductors.

The synthesis of MoS_2 begins with the deposition of Mo metal on SiO_2/Si or a quartz wafer by e-beam evaporation. The thickness of the molybdenum metal layer was varied from 0.5 to 3 nm using a deposition rate below ~0.1 Å s^{-1} under high vacuum conditions. The sample was positioned in the tubular quartz chamber represented in Fig. S1† under a rough vacuum (3.4×10^{-3} Torr) and heated up to 750 °C within a few seconds under the flow of Ar at a rate of 50 standard cubic centimeters per minute (sccm). In a pre-deposited sample, the surface of the molybdenum metal usually becomes oxidized under the atmospheric conditions. Such surfaces could be reduced by instantaneous reaction with hydrogen gas after reaching a temperature of 750 °C. After the pre-annealing process, the $H_2S/H_2/Ar$ (1 : 5 : 50) reaction gas mixture was injected to synthesize MoS_2 over 15 min. The chamber pressure was maintained at 3.1×10^{-1} Torr during the synthesis step. Instantaneous annealing at 1000 °C was found to enhance the crystallinity of MoS_2 films synthesized under a H_2S/Ar (1 : 50) gas mixture flow.[27] The sample was rapidly cooled down to room temperature by moving of the furnace from the reaction position under an Ar flow rate of 50 sccm.

The synthesized MoS_2 films were transferred onto a desired substrate using polymer supports, such as poly(methyl methacrylate) (PMMA), polydimethylsiloxane (PDMS), and thermal release tape (TRT), by etching away a SiO_2 sacrificial layer using buffered oxide etchant (BOE). After etching of the SiO_2 layer, polymer/MoS_2 was delivered onto a target substrate. The PMMA support layer was effectively removed using acetone boiled up to 80 °C. The TRT support was detached by removing the attractive force holding the MoS_2 when the 90 °C thermal treatment was performed using a roll to roll laminator.

Raman spectra and photoluminescence (PL) were obtained by confocal Raman microscopic systems (Witec Alpha 300 M+). Wavelength and power of the laser are 532 nm and 2 mW, respectively. Gratings of the spectrometer were 1800 and 600 g

mm^{-1} for Raman spectra and PL, respectively. The confocal Raman mapping images were obtained by calculating the difference between center values of Lorentz fitting to each Raman mode. UV-vis spectroscopy measurement for a number of layers was conducted with injection of a light source from a deuterium and tungsten lamp (Shimazu UV-3600). The information of binding energies in MoS_2 was characterized by using an X-ray photoelectron spectrometer (XPS, Phi V5000). XPS measurements were performed with an Al Kα X-ray source on the samples. The energy calibrations were made against the C 1s peak to eliminate the charging of the sample during analysis. The TEM samples were prepared using the transfer process of 2-layered MoS_2 onto the Cu grid. To avoid residue on the top surface of MoS_2, a polymer support layer was not employed in this process. TEM images were taken by using a FEI Titan Cube with acceleration voltage of 80 kV.

The 4-layered MoS_2 film was transferred onto an SiO_2/Si substrate which includes Au source and drain electrodes. The channel area was defined by the photolithography process with oxygen reactive ion etching. After fabricating the bottom gate structure, the device was annealed to improve contact resistance between MoS_2 and Au. Then a 30 nm HfO_2 layer was deposited on the entire area by the atomic layer deposition (ALD) process. TDMAH was used as an Hf precursor and H_2O was used as an oxidant. The substrate temperature was maintained at 250 °C during the entire ALD process. A top gate electrode overlapping the whole channel area was formed by thermal evaporation with the lift off pattern made by the photoresist.

Fig. 1 illustrates the mechanism of synthesis and transfer of the large-area MoS_2 film. The injected H_2S gas, which was used as a sulfur precursor, decomposed more readily than the evaporated solid sulfur source because the solid sulfur was evaporated at an even lower temperature, thus maintaining the aggregated states until adsorption onto the metal source. These processes resulted in poor film thickness uniformity.[22] However, H_2S precursor gas may be homogeneously adsorbed onto and reacted with the molybdenum surface without inducing aggregation, thus resulting in uniform quality of MoS_2 films. A sufficiently long sulfurization time under H_2S gas flow at 750 °C can result in the entire conversion of molybdenum into a MoS_2 layer; therefore, the synthesized layer thickness could be effectively controlled according to the thickness of the pre-deposited molybdenum layer. The synthesized film manifests an atomically flat surface indicated by the RMS surface roughness value of ~0.20 nm from atomic force microscopy
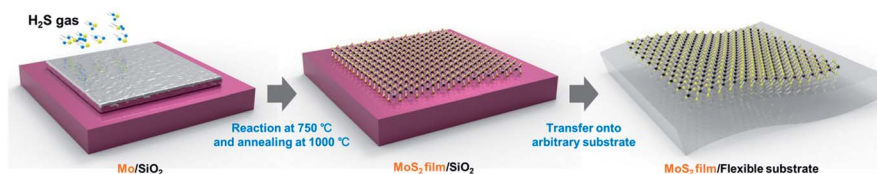
Fig. 1 Schematic illustration of the growth and transfer process system used to prepare MoS_2 films. Large-area MoS_2 films could be synthesized on a SiO_2/Si wafer or a quartz substrate using chemical vapor deposition processes, and the film could be transferred to an arbitrary substrate using a transfer process with a polymer support.

(AFM) (see Fig. S2†). The change of the sulfur precursor from solid sulfur[22] to H_2S gas, which can be considered as an incremental modification, was critical in making such a difference of almost perfect uniformity and precise thickness control of the synthesized film.

The synthesized MoS_2 film was uniformly transferred to a two-inch wafer substrate without creating visible cracks or wrinkles (Fig. 2a). Optical microscopy images of a 2 layer MoS_2 film on a SiO_2/Si substrate revealed a uniform color distribution (Fig. 2b). Transferred MoS_2 films do not show surface residue which could be originated from sulfuric precursors for the synthesis process and polymer supports for the transfer process. Fig. 2c and d show MoS_2 films on a transparent quartz substrate and a PET film. Transparent MoS_2 films were formed on quartz substrates by direct synthesis or on a plastic substrate by a wet transfer process. The letters "M", "o", "S", and "2" in Fig. 2a were formed from 2, 4, 8, and 12 layers of the MoS_2 film, respectively, which were offset against a dark level background. Once a molybdenum metal layer with 0.5, 1, 2, or 3 nm thickness had been deposited in the shape of the corresponding character, a MoS_2 film having a distinct number of layers could be synthesized by controlling the layer deposition mechanism, as described above. The synthesis result reveals that each layer of MoS_2 is synthesized from 0.25 nm of Mo metal. The MoS_2 films on the quartz substrates exhibited a high transparency, even for a 12 layer sample. The film prepared on the plastic substrate, which was formed from 4 layers, displayed a high flexibility. This suggests that even thick MoS_2 could be used in transparent and flexible electronics for the development of future device applications.

The qualities of the synthesized MoS_2 films having different numbers of layers were characterized using optical analysis methods, including Raman, photoluminescence (PL), and UV-vis spectroscopy. The Raman spectra revealed the peak

positions of the E_{2g}^1 and A_g^1 modes corresponding to in-plane and out-of-plane vibrations, as a function of the number of layers, respectively (Fig. 3a). The positions of the E_{2g}^1 and A_g^1 modes in the MoS_2 film were determined based on the vibrational energies of each mode, which were affected by the number of layers present. In general, the E_{2g}^1 vibration softened, whereas the A_g^1 vibration stiffened at higher numbers of layers. These trends allowed the shift in the Raman frequencies of each mode to be used as indicators of the number of layers present.[28] According to the spectra shown in Fig. 3a, the relative peak position differences between the modes varied from 20 to 26 cm^{-1}, which corresponded to 2 to 12 layered MoS_2 films, according to a previous study.[28,29] The PL response in the energy range corresponding to a direct transition indicated semiconducting behavior in the $2H\text{-}MoS_2$ films.[30,31] In general, the relative intensity of the PL band decreased as the number of MoS_2 layers present increased because the indirect electron transitions dominated the direct transitions. The direct electron transition wavelength was shifted to higher values at higher numbers of MoS_2 layers.[30] The PL response of the synthesized MoS_2 film was represented by the intensity decay. The transition wavelength was red-shifted in samples having a higher number of layers (Fig. 3b). Fig. 3c shows the UV-vis transmittance spectra of 2, 4, 8, and 12 layered MoS_2 films. The peak positions in each MoS_2 film corresponded to the band structure. The peak positions shifted to lower energies as the number of layers in the PL spectra increased.[31] The transmittance values in the visible region (550 nm) were 96.7% (2 layers), 89.2% (4 layers), 69.4% (8 layers), and 48.4% (12 layers). These values were inversely proportional to the number of layers.

The crystal lattice structure and quantity of the residual, unreacted Mo metal present were characterized using XPS techniques (Fig. 4a). In general, hetero-atomic bonds involving Mo atoms yield bonding energies that depend on the crystal structure and atomic composition. $1T\text{-}MoS_2$ and $2H\text{-}MoS_2$ displayed different binding energies for each orbital in the Mo and S centers, yielding, respectively, metallic or semiconducting behavior. The $2H\text{-}MoS_2$ sample displayed a shift in the Mo orbital binding energy to 229.5 and 232.6 eV, which corresponded to the Mo $3d_{5/2}$ and Mo $3d_{3/2}$ orbitals, respectively.[32] The negligible peak intensity at the initial binding energy of the Mo orbital indicated that complete sulfurization of the Mo atoms had taken place to form the $2H\text{-}MoS_2$ crystalline structure. The binding energies of the S atom orbitals further supported the formation of the $2H\text{-}MoS_2$ crystal structure. Therefore, the MoS_2 sample synthesized using this method exhibited a completely sulfurized lattice that had been converted to a 2H-structure without yielding residual Mo atoms or a 1T-structured MoS_2 phase.[30] The concentration of MoO_3 in the MoS_2 lattice is important because these moieties can act as trap centers for charge carriers passing through the MoS_2 layer. The negligible intensity of the MoO_3 binding energy peak at 232.8 and 235.6 eV indicated that the low pressure and the Ar/H_2 atmosphere prevented the formation of MoO_3 during the synthesis process.[33]

A more detailed structural analysis was performed using high-resolution TEM (HRTEM). The HRTEM image shown in
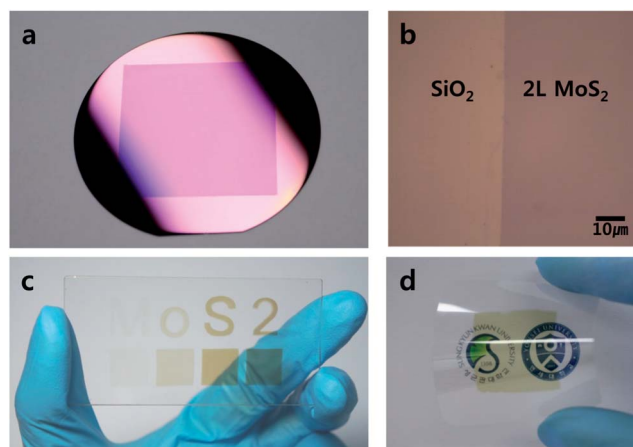
Fig. 2 Large-area, uniform MoS_2 films prepared on different substrates. (a) Wafer-scale MoS_2 films synthesized by CVD processes and transferred using a polymer support. (b) Microscopic image of a uniform 2-layered MoS_2 film. (c) The characters 'M', 'o', 'S', and '2' were prepared from 2, 4, 8, and 12 layered MoS_2 films, respectively. (d) MoS_2 film transferred onto a PET substrate, demonstrating mechanical bendability.
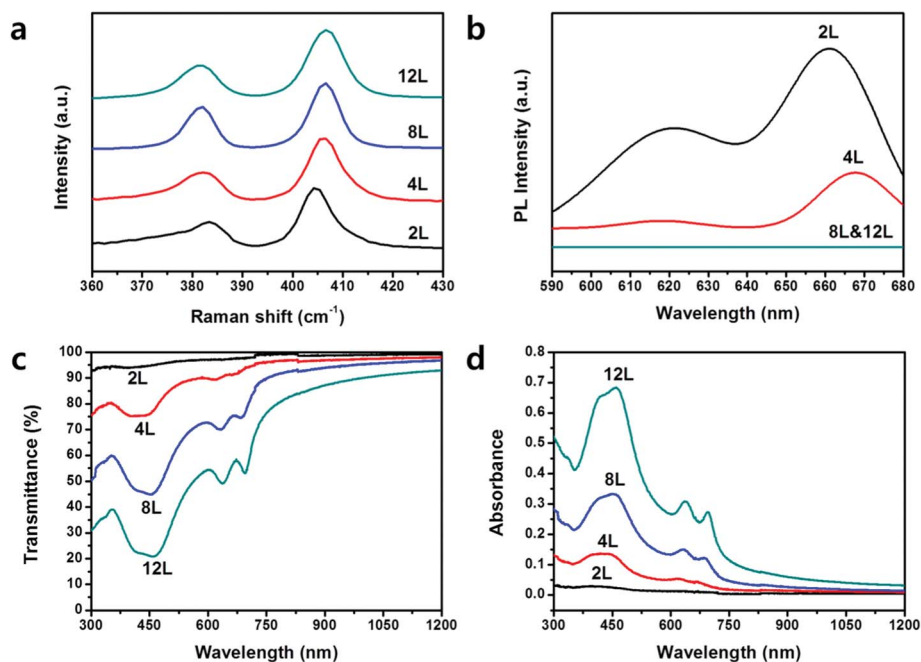
Fig. 3 Optical characterization of films prepared with different layer numbers. (a) The Raman spectra of the MoS_2 films prepared with layers increasing from 2 to 12. (b) Photoluminescence spectra of the MoS_2 films having different thickness values using a 532 nm excitation laser. (c and d) UV-vis transmittance and absorbance spectra of the MoS_2 films as a function of the layer number.
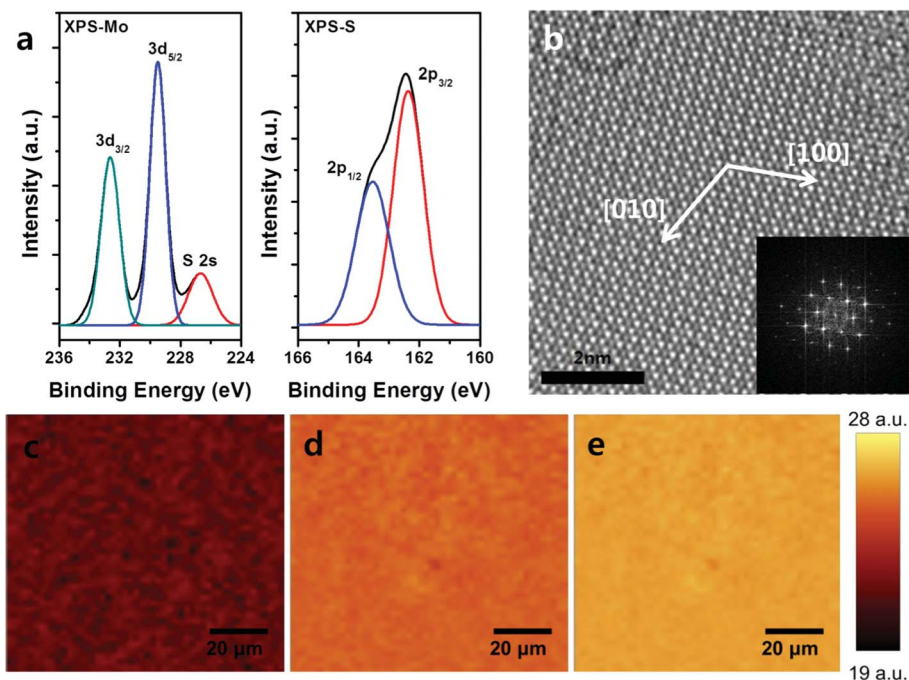
Fig. 4 Structural characterization of the synthesized films. (a) X-ray photoluminescence spectroscopy (XPS) was used to analyze the binding energies of the Mo and S atoms in the synthesized MoS_2 film. (b) High-resolution transmission electron microscopy (HRTEM) images of the synthesized MoS_2 film (the inset shows the diffraction pattern of the electron-transmitting area). (c–e) Confocal Raman microscopy images of the 2-, 4-, and 12-layered MoS_2 films representing a large-area uniform distribution.

Fig. 4b indicates a high crystallinity in the synthesized MoS_2 film, which was also inferred from the corresponding diffraction pattern shown in the inset of Fig. 4b. The diffraction patterns indicated a crystalline direction indicated by the arrow in Fig. 4b. 2H-Structured synthesis appeared to proceed along the planar direction. The crystalline domain size in the synthesized MoS_2 films was determined to be around 10 nm based on the HRTEM images (see Fig. S3†).

The controllability over the number and uniformity of the layers was examined by conducting Raman mapping studies over a few hundred micrometers in the synthesized 2, 4, and 12 layered MoS_2 films. Fig. 4c–e show two-dimensional Raman maps of the peak position differences between the A_g^1 and E_{2g}^1 modes for three different MoS_2 films having different thickness values. The color distributions in the Raman mapping images showed almost perfect uniformity over the large areas. These results indicated that the synthesis method described here can provide highly uniform thickness-controlled films.

The surface morphologies were characterized using AFM techniques, and the roughness values were found to be comparable to the values for the substrate itself. The thickness variation was found to be negligible, indicating that the films were highly uniform, as revealed in the Raman spectroscopy measurements. The number of layers of the film was checked again by using AFM. The measured step heights of 2L, 4L, 8L, and 14L of MoS_2 films corresponded to the theoretical thicknesses, revealing that the results agreed with the Raman spectroscopy measurements (see Fig. S4†).

Top-gated TFT-arrays (∼4000 devices) were fabricated using a 4 layered MoS_2 film as the channel material, mounted on a 2 inch SiO_2/Si substrate and prepared using conventional photolithography and etching processes (Fig. 5a). The device arrays were prepared with a variety of channel geometries, where the length was varied from 10 to 25 μm and the width was varied from 100 to 200 μm. Source–drain (S–D) and gate (G) contact electrodes were formed by evaporating the Au metal.

A gate dielectric layer comprising a 30 nm thick HfO_2 layer was deposited using atomic layer deposition (ALD) methods. The devices were annealed to enhance the electrical contact at 300 °C in a vacuum environment. Fig. 5b and c show the electrical characteristics of a representative device having a channel length of 15 μm and a width of 200 μm. The electron mobility and the on/off current ratio were 0.12 cm^2 V^{-1} s^{-1} and 10^5 respectively. The linearity of the I_{ds}–V_{ds} characteristic curves indicated ohmic contact between the film and the electrodes. Fig. 5d shows a statistical distribution of the electron mobilities measured in an array of 180 FET devices. Over 90% of all devices exhibited stable operation, with a mean value of 0.07 cm^2 V^{-1} s^{-1}. The low mobility and failure of the devices appeared to be due to the small crystal domain size and the boundary properties, which may act as charge scatterers. We speculate that by controlling annealing time, annealing environment, or the substrate material the film quality can be improved.

In conclusion, we demonstrated the large-area synthesis of uniform and transparent MoS_2 films, with control over the number of synthesized layers, using CVD methods involving gas and metal precursors. The thickness of the synthesized MoS_2 film could be controlled by depositing Mo layers having different thickness values. The synthesized MoS_2 films were characterized by Raman/PL/UV-vis spectroscopy, AFM, XPS, and HRTEM. All analyses revealed almost perfect film uniformity, precisely controlled film thickness values, and high film crystallinity without the presence of an amorphous phase. TFT arrays prepared from the synthesized films were used to
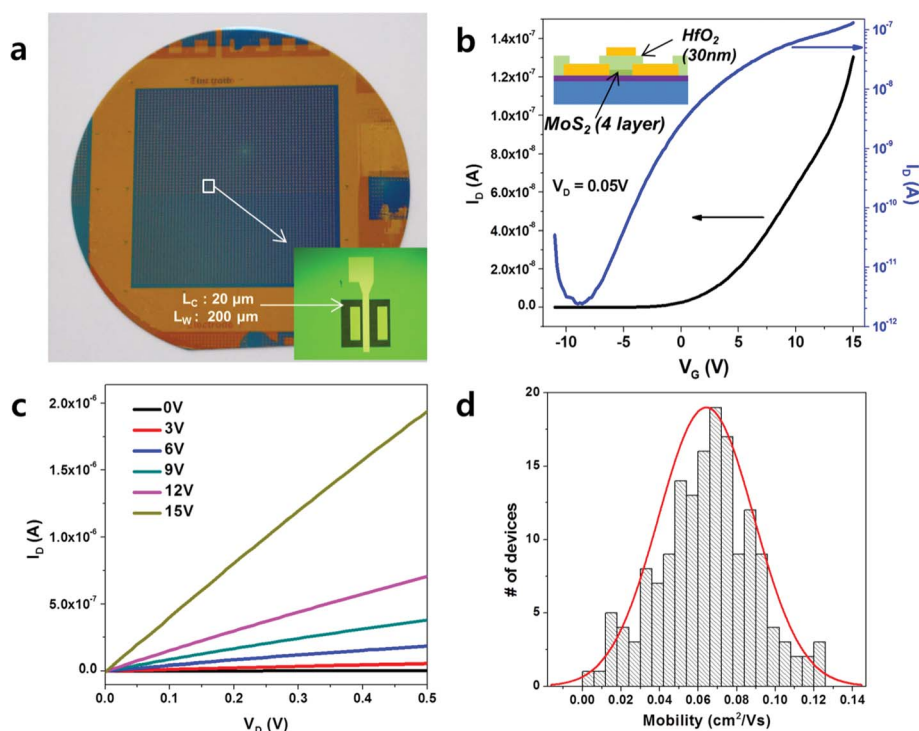
Fig. 5 Electrical characterization of the arrays of MoS_2 FET devices. (a) Photographic image of a MoS_2 top-gate transistor array on a two-inch SiO_2/Si wafer. (b) Transport characteristics of top-gate MoS_2 devices under a drain voltage of 50 mV. The inset denotes the device cross-section. (c) The output characteristics of the top-gate CVD-MoS_2 devices under various gate bias values. (d) Histogram of the mobility distributions obtained from the large-area MoS_2 devices.

demonstrate the stable operation of devices (>90% stability), with a mobility of 0.12 cm^2 V^{-1} s^{-1} for the best devices and a high on/off current ratio of 10^5. We judge that use of the gas phase sulfur precursor is the key factor to thickness controllability and film uniformity. This synthesis method may be applied to other types of metal chalcogenides. The films are useful for the preparation of large-area devices, such as thin film transistors for use in transparent and/or flexible displays, sensors, and solar cells.

Acknowledgements

References

1 K. S. Novoselov, D. Jiang, F. Schedin, T. J. Booth, V. V. Khotkevich, S. V. Morozov and A. K. Geim, *Proc. Natl. Acad. Sci. U. S. A.*, 2005, **102**, 10451–10453.

2 C. Lee, X. D. Wei, J. W. Kysar and J. Hone, *Science*, 2008, **321**, 385–388.

3 A. Castellanos-Gomez, M. Poot, G. A. Steele, H. S. J. van der Zant, N. Agrait and G. Rubio-Bollinger, *Adv. Mater.*, 2012, **24**, 772–775.

4 C. R. Dean, A. F. Young, I. Meric, C. Lee, L. Wang, S. Sorgenfrei, K. Watanabe, T. Taniguchi, P. Kim, K. L. Shepard and J. Hone, *Nat. Nanotechnol.*, 2010, **5**, 722–726.

5 K. S. Novoselov, A. K. Geim, S. V. Morozov, D. Jiang, M. I. Katsnelson, I. V. Grigorieva, S. V. Dubonos and A. A. Firsov, *Nature*, 2005, **438**, 197–200.

6 K. S. Novoselov, A. K. Geim, S. V. Morozov, D. Jiang, Y. Zhang, S. V. Dubonos, I. V. Grigorieva and A. A. Firsov, *Science*, 2004, **306**, 666–669.

7 Y. B. Zhang, Y. W. Tan, H. L. Stormer and P. Kim, *Nature*, 2005, **438**, 201–204.

8 A. H. Castro Neto, F. Guinea, N. M. R. Peres, K. S. Novoselov and A. K. Geim, *Rev. Mod. Phys.*, 2009, **81**, 109–162.

9 K. F. Mak, M. Y. Sfeir, Y. Wu, C. H. Lui, J. A. Misewich and T. F. Heinz, *Phys. Rev. Lett.*, 2008, **101**, 196405.

10 A. C. Ferrari, J. C. Meyer, V. Scardaci, C. Casiraghi, M. Lazzeri, F. Mauri, S. Piscanec, D. Jiang, K. S. Novoselov, S. Roth and A. K. Geim, *Phys. Rev. Lett.*, 2006, **97**, 187401.

11 F. Bonaccorso, Z. Sun, T. Hasan and A. C. Ferrari, *Nat. Photonics*, 2010, **4**, 611–622.

12 V. C. Sanchez, A. Jachak, R. H. Hurt and A. B. Kane, *Chem. Res. Toxicol.*, 2012, **25**, 15–34.

13 A. K. Geim, *Science*, 2009, **324**, 1530–1534.

14 K. I. Bolotin, K. J. Sikes, Z. Jiang, M. Klima, G. Fudenberg, J. Hone, P. Kim and H. L. Stormer, *Solid State Commun.*, 2008, **146**, 351–355.

15 F. Schwierz, *Nat. Nanotechnol.*, 2010, **5**, 487–496.

16 Y. W. Son, M. L. Cohen and S. G. Louie, *Nature*, 2006, **444**, 347–349.

17 D. C. Elias, R. R. Nair, T. M. G. Mohiuddin, S. V. Morozov, P. Blake, M. P. Halsall, A. C. Ferrari, D. W. Boukhvalov, M. I. Katsnelson, A. K. Geim and K. S. Novoselov, *Science*, 2009, **323**, 610–613.

18 R. Balog, B. Jorgensen, L. Nilsson, M. Andersen, E. Rienks, M. Bianchi, M. Fanetti, E. Laegsgaard, A. Baraldi, S. Lizzit, Z. Sljivancanin, F. Besenbacher, B. Hammer, T. G. Pedersen, P. Hofmann and L. Hornekaer, *Nat. Mater.*, 2010, **9**, 315–319.

19 J. W. Bai, X. Zhong, S. Jiang, Y. Huang and X. F. Duan, *Nat. Nanotechnol.*, 2010, **5**, 190–194.

20 Q. H. Wang, K. Kalantar-Zadeh, A. Kis, J. N. Coleman and M. S. Strano, *Nat. Nanotechnol.*, 2012, **7**, 699–712.

21 B. Radisavljevic, A. Radenovic, J. Brivio, V. Giacometti and A. Kis, *Nat. Nanotechnol.*, 2011, **6**, 147–150.

22 Y. J. Zhan, Z. Liu, S. Najmaei, P. M. Ajayan and J. Lou, *Small*, 2012, **8**, 966–971.

23 Y. H. Lee, X. Q. Zhang, W. J. Zhang, M. T. Chang, C. T. Lin, K. D. Chang, Y. C. Yu, J. T. W. Wang, C. S. Chang, L. J. Li and T. W. Lin, *Adv. Mater.*, 2012, **24**, 2320–2325.

24 K. K. Liu, W. J. Zhang, Y. H. Lee, Y. C. Lin, M. T. Chang, C. Su, C. S. Chang, H. Li, Y. M. Shi, H. Zhang, C. S. Lai and L. J. Li, *Nano Lett.*, 2012, **12**, 1538–1544.

25 Y. F. Yu, C. Li, Y. Liu, L. Q. Su, Y. Zhang and L. Y. Cao, *Sci. Rep.*, 2013, **3**, 1866.

26 Y. C. Lin, W. J. Zhang, J. K. Huang, K. K. Liu, Y. H. Lee, C. T. Liang, C. W. Chu and L. J. Li, *Nanoscale*, 2012, **4**, 6637–6641.

27 H. Hadouda, J. Pouzet, J. C. Bernede and A. Barreau, *Mater. Chem. Phys.*, 1995, **42**, 291–297.

28 C. Lee, H. Yan, L. E. Brus, T. F. Heinz, J. Hone and S. Ryu, *ACS Nano*, 2010, **4**, 2695–2700.

29 H. Li, Q. Zhang, C. C. R. Yap, B. K. Tay, T. H. T. Edwin, A. Olivier and D. Baillargeat, *Adv. Funct. Mater.*, 2012, **22**, 1385–1390.

30 G. Eda, H. Yamaguchi, D. Voiry, T. Fujita, M. W. Chen and M. Chhowalla, *Nano Lett.*, 2011, **11**, 5111–5116.

31 K. F. Mak, C. Lee, J. Hone, J. Shan and T. F. Heinz, *Phys. Rev. Lett.*, 2010, **105**, 136805.

32 C. A. Papageorgopoulos and W. Jaegermann, *Surf. Sci.*, 1995, **338**, 83–93.

33 J. G. Choi and L. T. Thompson, *Appl. Surf. Sci.*, 1996, **93**, 143–149.